<div align="center">Supplementary Information</div>

Polyiodide shuttle inhibition in ethylene glycol-added aqueous electrolytes for high energy and long-term cyclability of zinc-iodine batteries

Jing Zhang[1], Qingyun Dou[2, *], Chao Yang[1], Limin Zang[1, *], Xingbin Yan[2]

[1] *Guangxi Colleges and Universities Key Laboratory of Natural and Biomedical Polymer Materials, College of Materials Science and Engineering, Guilin University of Technology, Guilin 541004, China.*

[2] *Department of Materials Science and Engineering, Sun Yat-Sen University, Guangzhou 510275, China.*

---

[*] Corresponding authors. E-mail addresses: 2016034@glut.edu.cn (L. Zang), douqy3@mail.sysu.edu.cn (Q. Dou).

Materials

Natural flake graphite (325 mesh) was purchased from Qingdao Huatai Lubrication seal Technology Co., Ltd. Super P was purchased from Guangdong candlelight New Energy Technology Co., Ltd. Poly vinylidene fluoride (PVDF) was purchased from Dongguan Jinhu Plastic materials Co., Ltd. Potassium hydroxide (KOH), zinc iodide (ZnI_2) and Gelatin were purchased from Aladdin Co., Ltd. Ethylene glycol (EG), potassium permanganate ($KMnO_4$), sulfuric acid (H_2SO_4), hydrochloric acid (HCl), zinc sulfate heptahydrate ($ZnSO_4 \cdot 7H_2O$), N,N-Dimethylformamide (DMF), hydrogen peroxide(H_2O_2), and sodium nitrate ($NaNO_3$) were purchased from West Gansu Science Co., Ltd.

Preparation of high density ordered porous graphene (HOPG) [1]

The graphene oxide (GO) dispersion was prepared from natural flake graphite (325 mesh) by the modified Hummers method. Then 15 mL 0.2 M (mol L^{-1}) KOH solution was slowly added to 15 mL 6 mg mL^{-1} GO dispersion under magnetic stirring to obtain a long range ordered GO liquid crystal. The GO liquid crystal was sealed into a 100 mL Teflon-lined autoclave and heated at 180 °C for 6 h. The resultant hydrogel was thoroughly soaked with 1 M HCl to remove KOH, and then washed with deionized water until the solution is neutral. Finally, the hydrogel was subjected to capillary densification and dried in a vacuum oven at 55 °C for 12 h to afford HOPG.

High density disordered porous graphene (HDPG) was prepared by the same method as HOPG but without the addition of KOH solution into GO dispersion.

Cell fabrication and electrochemical measurement

The HOPG and HDPG cathodes was prepared by a coating method. Typically, the active material, super-P and PVDF binder were mixed evenly at a mass ratio of 8:1:1, and DMF was added as dispersant. The mixture was grinded to obtain a uniform slurry, which was then coated on the 300 mesh steel mesh by scraper and dried in a vacuum oven at 60 °C for 12 h. The sheet was pressed with a pressure of 10 MPa. The coin-type cells (LIR 2032) were assembled using HOPG or HDPG cathode, Zn anode, and filter paper separator in various electrolytes.

The cyclic voltammetry (CV), linear sweep voltammetry (LSV), galvanostatic charge/discharge (GCD), chronoamperometry (CA), and electrochemical impedance spectroscopy (EIS) measurements were conducted using an electrochemical workstation (CHI660E, Shanghai, China). The cycling stability measurements were conducted using a LAND test system (CT3002A, Wuhan Land Electronic Co. Ltd).

Material characterization

The surface morphology was investigated by using a scanning electron microscopy (SEM, Hitachi S-4800, Japan). The chemical structure and composition were analyzed by Raman spectroscopy (Thermo Scientific™ DXR, USA), X-ray diffractometer (XRD, Model X′pert PRO, PANalytical, Netherlands), X-ray photoelectron spectroscopy (XPS, Thermo Scientific™ K-Alpha™+), Fourier-transform infrared spectrometer (FT-IR, Nexus 470FT-IR, Nico Let, USA), polarizing microscope (POM, Cai Kang CK-300, China), surface area test method (BET, Baster 3H-2000PM2, China), contact angle goniometer (Jinhe JY-PHb, China), atomic force microscope (AFM, NT-MDT NTEGRA Russia), ultraviolet spectrophotometer (UV-vis, UV-9000S, Shanghai Yuan Instrument Co., LTD), ^{1}H Nuclear Magnetic Resonance (^{1}H NMR, AVANCE NEO 400MHZ), and X-ray photoelectron spectroscopy (XPS, Thermo Scientific ESCALAB 250Xi, USA).

Molecular dynamics (MD) simulations

Classical MD simulations were perform using the Forcite module in Materials Studio. The forced field parameters were obtained from Condensed Molecular potential for Atomistic Simulation Studies (COMPASS) force fields. Amorphous Cell module was used to construct 2 M $ZnSO_4$+0.2 M ZnI_2/H_2O+20% EG box containing 1110 H_2O, 55 Zn^{2+}, 50 SO_4^{2-}, 10 I^-, and 90 EG, and 2 M $ZnSO_4$+0.2 M ZnI_2/H_2O box containing 1112 H_2O, 44 Zn^{2+}, 40 SO_4^{2-}, 8 I^-.

Electrochemical calculation

The gravimetric capacities of electrodes are calculated from the GCD curves using the following calculation formula:

$$C_g = \frac{I \cdot \Delta t}{3.6m} \tag{1}$$

where I (A) is the discharge current, Δt (s) is the discharge time, m (g) is the mass of the active material.

The volumetric capacities of electrodes are calculated by the following formula:

$$C_V = \rho \cdot C_g \tag{2}$$

where ρ (g cm^{-3}) is the density of the electrode material.

The energy densities can be calculated by the following formula:

$$E_{Vol} = \frac{I \int_{t(V\max)}^{t(V\min)} V(t).dt}{3.6m} \cdot \rho \tag{3}$$

The corresponding power densities are calculated by the following formula:

$$P_{Vol} = \frac{E \cdot 3600}{\Delta t} \tag{4}$$

where Δt (s) is the corresponding discharge time.
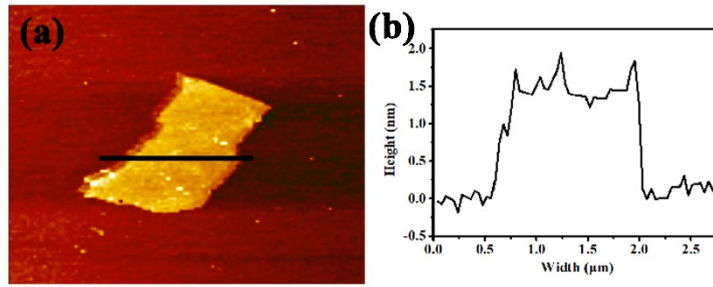
Figure S1. (a) AFM image of GO sheet. (b) GO thickness scan curve.
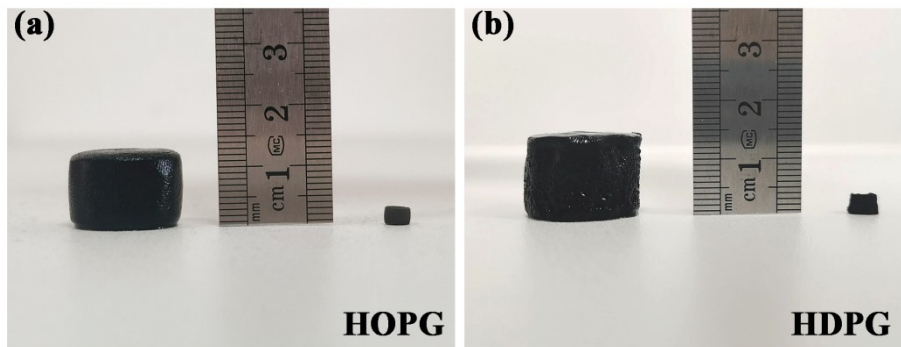
Figure S2. (a, b) Photographs of HOPG (a) and HDPG (b) before and after capillary densification.
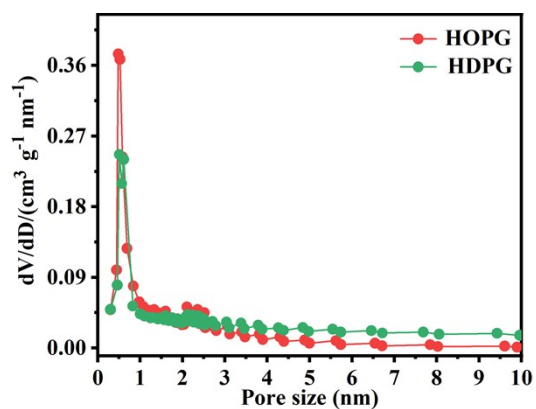
Figure S3. Pore size distribution (PSD) curves of HOPG and HDPG.

Table S1. Physical properties of HOPG and HDPG samples.

Samples	BET surface area ($m^2 \, g^{-1}$)	Total pore volume ($cm^3 \, g^{-1}$)	Micropore volume ($cm^3 \, g^{-1}$)	Mesopore volume ($cm^3 \, g^{-1}$)	Densities ($g \, cm^{-3}$)
HOPG	333	0.22	0.17	0.05	1.4
HDPG	209	0.20	0.12	0.08	1.08
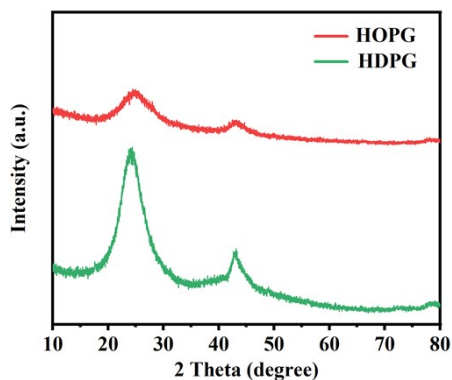
Figure S4. XRD patterns of HOPG and HDPG.
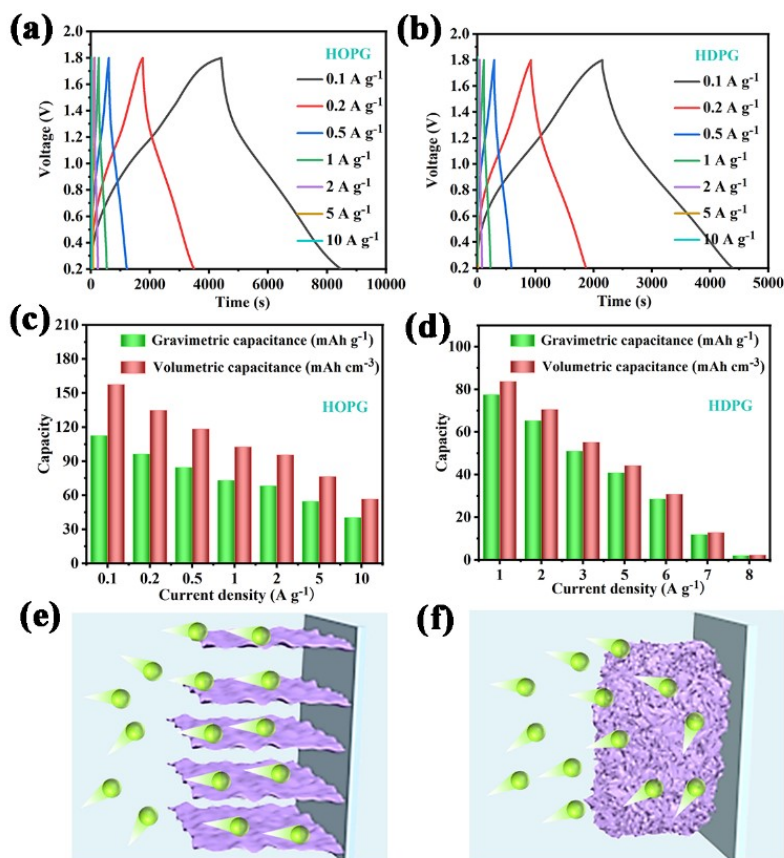
Figure S5. (a, b) GCD curves at different scan rates for HOPG (a) and HDPG (b). (c, d) Gravimetric and volumetric capacities at different current densities for HOPG (c) and HDPG (d). (e, f) Schematic showing the working mechanisms of HOPG (e) and HDPG (f).
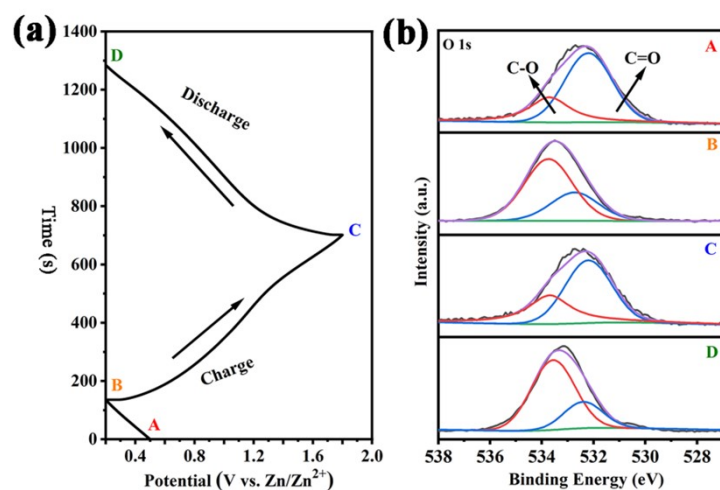
Figure S6. (a) GCD curve at 0.5 A g^{-1} for HOPG. (b) Ex-situ O 1s XPS spectra of HOPG at different charging/discharging states as marked in (a).
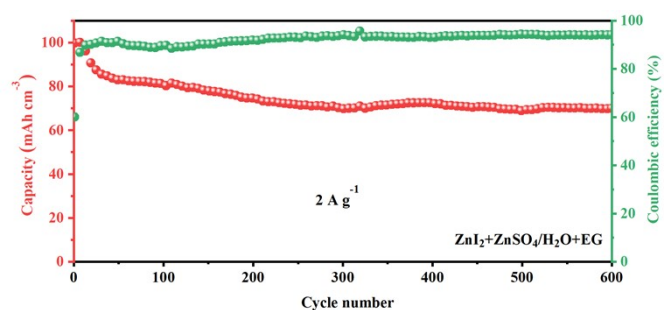

Figure S7. Cycling stability at 2 A g^{-1} for the cell using HDPG cathode and Zn anode in ZnI$_2$+ZnSO$_4$/H$_2$O+EG electrolyte.
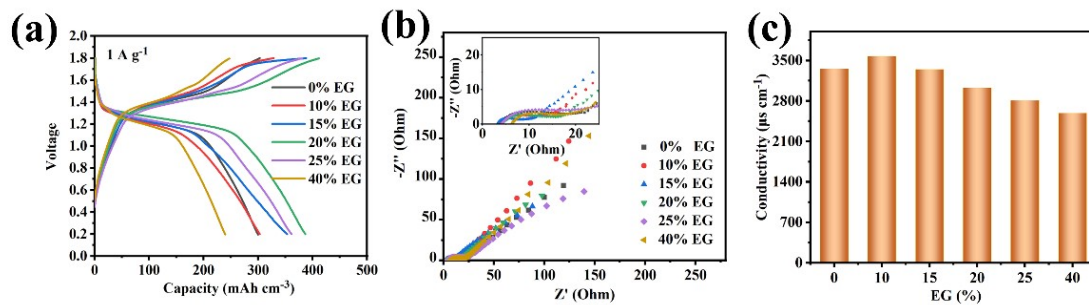
Figure S8. (a) GCD cures at 1A g^{-1} and (b) Nyquist plots for the cells using ZnI_2+ZnSO_4/H_2O+EG electrolytes with different EG volume fractions. (c) Conductivities of ZnI_2+ZnSO_4/H_2O+EG electrolytes with different EG volume fractions.
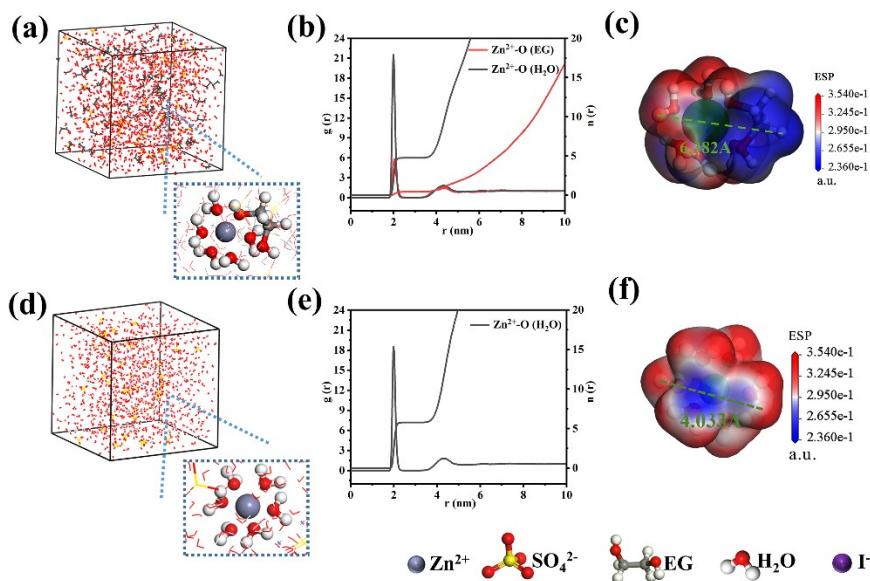
Figure S9. (a, d) 3D snapshots of $ZnSO_4+ZnI_2/H_2O+EG$ solution (a) and $ZnSO_4+ZnI_2/H_2O$ solution (d) obtained from MD simulations. (b, e) Radial distribution functions for $Zn^{2+}-O$ (H_2O) and $Zn^{2+}-O$ (EG) in $ZnSO_4+ZnI_2/H_2O+EG$ solution (b) and for $Zn^{2+}-O$ (H_2O) in $ZnSO_4+ZnI_2/H_2O$ solution (e). (c, f) Electrostatic potential mapping of $EG-Zn^{2+}-5H_2O$ in $ZnSO_4+ZnI_2/H_2O+EG$ solution (c) and $Zn^{2+}-6H_2O$ in $ZnSO_4+ZnI_2/H_2O$ solution (f).
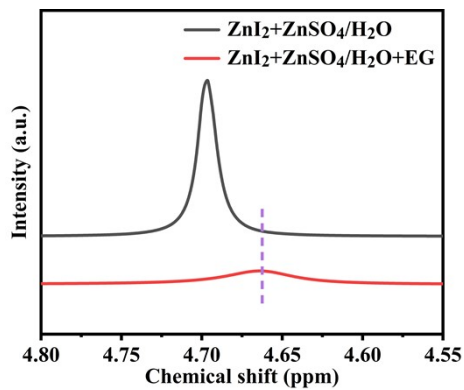
Figure S10. ^1H NMR spectra for $ZnSO_4+ZnI_2/H_2O+EG$ and $ZnSO_4+ZnI_2/H_2O$ solutions.
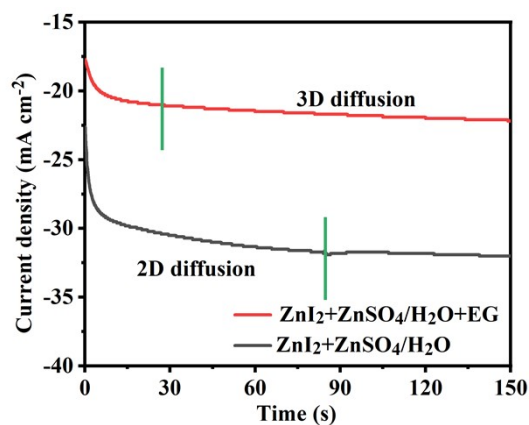

Figure S11. CA polarization curves with an applied overpotential of 15 mV tested in three-electrode cells with Zn working electrode, copper counter electrode, Ag/AgCl reference electrode, in $ZnSO_4+ZnI_2/H_2O$ and $ZnSO_4+ZnI_2/H_2O+EG$ electrolytes.
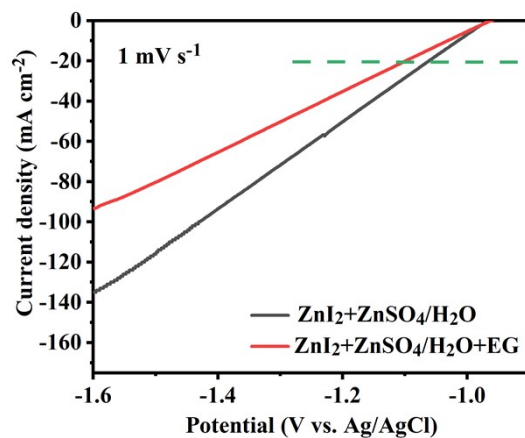
Figure S12. LSV curves at 1 mV s^{-1} tested in three-electrode cells with Zn working electrode, platinum counter electrode, Ag/AgCl reference electrode, in ZnSO$_4$+ZnI$_2$/H$_2$O and ZnSO$_4$+ZnI$_2$/H$_2$O+EG electrolytes.
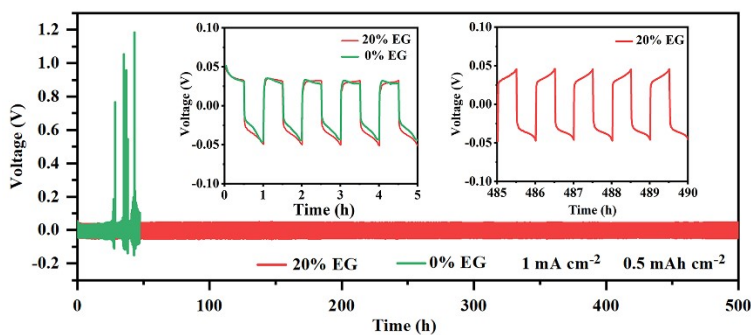
Figure S13. Potential profiles for the of Zn//Zn symmetric cells in ZnSO$_4$+ZnI$_2$/H$_2$O and ZnSO$_4$+ZnI$_2$/H$_2$O+EG solutions cycled under 1.0 mA cm^{-2} and 0.5 mA h cm^{-2}.
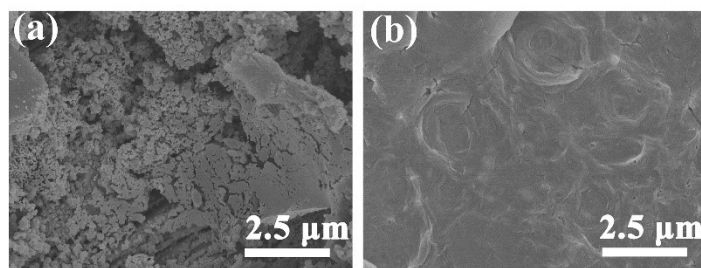
Figure S14. (a, b) SEM images of Zn electrodes after 25 h cycles in ZnSO$_4$+ZnI$_2$/H$_2$O solution (a) and ZnSO$_4$+ZnI$_2$/H$_2$O+EG solution (b).

Table S2. Comparison of energy densities of carbon-based materials

Cathode	Anode	Electrolyte	Voltage	Energy Density (Wh L^{-1})	Power density (W L^{-1})	Carbon Density (g cm^{-3})	Reference
HOPG	Zn	ZnSO$_4$/ZnI$_2$	0.2−1.8	334.3	1517.6	1.4	This work
HOPG	Zn	ZnSO$_4$	0.2−1.8	126	112	1.4	This work
HOPC	Zn	ZnSO$_4$	0.2−1.8	139.2	1515.2	1.48	2
3D-PG-1	Zn	Zn(OTf)$_2$	0.2−1.8	96.8	1187.7	1.38	3
NHG-rGO	Zn	ZnCl$_2$	0.2−1.7	75	76.7		4
DGH	Zn	ZnSO$_4$	0.2−1.8	108.6	1180.1	1.5	5
Diamond fibers	Zn	ZnSO$_4$	0.2−1.8	220	2229.8		6
FCNSs	Zn	Zn(OTf)$_2$/IL	0−2.4	54.3	27.5		7
AC	Zn	ZnSO$_4$	0.2−1.8	7.4	13.1		8
rGO/CNT	Zn	ZnSO$_4$	0−1.8	48.5	179.9		9

References

1 H. Ma, H. Geng, B. Yao, M. Wu, C. Li, M. Zhang, F. Chi, L. Qu, *ACS Nano*, 2019, 13, 9161-9170.

2 H. Ma, H. Chen, M. Wu, F. Chi, F. Liu, J. Bai, H. Cheng, C. Li, L. Qu, *Angew. Chem. Int. Ed.*, 2020, 59, 14541-14549.

3 X. Xu, X. Zhao, Z. Yang, Q. Lin, B. Jian, N. Li, C. Zheng, W. Lv, *Carbon*, 2022, 186, 624-631.

4 J. Luo, L. Xu, H. Liu, Y. Wang, Q. Wang, Y. Shao, M. Wang, D. Yang, S. Li, L. Zhang, Z. Xia, T. Cheng, Y. Shao, *Adv. Funct. Mater.*, 2022, 32, 2112151.

5 L. Zhang, D. Wu, G. Wang, Y. Xu, H. Li, X. Yan, *Chin Chem Lett*, 2021, 32, 926-931.

6 Z. Jian, N. Yang, M. Vogel, S. Leith, A. Schulte, H. Schönherr, T. Jiao, W. Zhang, J. Müller, B. Butz, X. Jiang, *Adv. Energy Mater.*, 2020, 10, 2002202.

7 H. Zhou, C. Liu, J.C. Wu, M. Liu, D. Zhang, H. Song, X. Zhang, H. Gao, J. Yang, D. Chen, *J. Mater. Chem. A*, 2019, 7, 9708-9715.

8 L. Dong, X. Ma, Y. Li, L. Zhao, W. Liu, J. Cheng, C. Xu, B. Li, Q.H. Yang, F. Kang, *Energy Storage Mater.*, 2018, 13, 96-102.

9 X. Zhang, Z. Pei, C. Wang, Z. Yuan, L. Wei, Y. Pan, A. Mahmood, Q. Shao, Y. Chen, *Small*, 2019, 15, 1903817.